

We are IntechOpen, the world's leading publisher of Open Access books Built by scientists, for scientists

4,800

Open access books available

122,000

International authors and editors

135M

Downloads

Our authors are among the

154

Countries delivered to

TOP 1%

most cited scientists

12.2%

Contributors from top 500 universities



WEB OF SCIENCE™

Selection of our books indexed in the Book Citation Index
in Web of Science™ Core Collection (BKCI)

Interested in publishing with us?
Contact book.department@intechopen.com

Numbers displayed above are based on latest data collected.

For more information visit www.intechopen.com



Issues in Solid-State Physics

Roberto Raúl Deza

Abstract

In the first sections, we bring into the present context some of our past contributions on the influence of quantum correlations on the formation of tightly bound solids. We discuss the effects of the overlap between neighbor orbitals in diverse situations of interest—involving both bulk and surface states—and call the reader's attention to an exact tight-binding calculation which allows gauging the errors introduced by the underlying hypotheses of the usual tight-binding approximation. We round up this part by reviewing a quantum Monte Carlo method specific for strongly correlated fermion systems. In the last section, we explore some non-equilibrium routes to (not necessarily tightly bound) solid state: we discuss spatio-temporal pattern formation in arrays of FitzHugh-Nagumo (FHN) neurons, akin to resonant crystal structures.

Keywords: quantum correlations, band structure, tight-binding approach, neighbor orbital overlap, fermion Monte Carlo, non-equilibrium pattern formation, spatiotemporal synchronization

1. Introduction

Since childhood, we all have an intuition of what a solid is. However, most properties we intuitively assign to solids come in a vast range. Diamonds—and some metals—are hard, and ordinary glasses are brittle; but vulcanized rubber is neither, and it is a solid too. Perhaps the best characterization is this: *at our human timescales, a solid does not flow*. That is why this category includes glasses and ice (which do flow but at least at geological timescales).

Regarding their structure, a huge class of solids are *crystalline*. This is so to such extent that *solid state* came to be synonymous of crystalline structure, and the more comprehensive category of *condensed matter* (which admittedly includes condensed fluids or liquids) came into fashion. The name *crystal* was assigned in the late antiquity to precious and semiprecious stones that outstood for their transparency and diaphaneity. In fact, the modern meaning of the term as “an almost perfectly ordered structure” explains easily those properties.¹

Many solids we interact with—metals, stones, etc.—are random assemblies of grains, held together by strong adhesion forces. Like those of sand, quartz, or salt, those grains are very likely to be themselves crystals (which as said do not imply they are perfect: they may contain lots of impurities and defects). But there are two particular aspects of crystals we are concerned with here. The first is that

¹ For isolators like these, the bandgap is too large for visible light to be absorbed by creating electron-hole pairs. Moreover, the absence of charge carriers rules out light scattering. Impurities provide localized midgap states, which favor two-step electron-hole pair creation by visible light.

unlike complex systems, which may display emergent structures at each scale (think, e.g., of mitochondria, cells, tissues, organs, etc.), crystals are very simple: they are huge assemblies of elementary building blocks (be they atoms, molecules, nanoclusters, or whatever). The second is that since the building blocks obey quantum mechanics, crystals inherit the quantum character (despite being themselves macroscopic).

As recent experiments have shown, whereas most interactions (but gravity) are effectively short-ranged, there is no limit for quantum correlations; and this fact makes them the most important fact to account for in modeling. Quantum correlations manifest themselves in many ways, but the by far dominant one comes from the indistinguishability of identical particles. Unless the crystal is a monolayer, the state vector of a system of many indistinguishable particles must be either *totally symmetric* or *totally antisymmetric* (a determinant) under exchange. In the first case, the particles obey Bose-Einstein statistics and are called *bosons*. In the second, the particles obey Fermi-Dirac statistics and are called *fermions*. The requirement that the state vector of a system with many fermions be totally antisymmetric is the celebrated *exclusion principle*, postulated by Pauli.

At present, there is no question that atoms are distinguishable. They can even be individually manipulated.² Since in modeling crystals, it suffices to take atoms as building blocks (we resolve up to the nanoscale), it does not matter that they are themselves composed of other indistinguishable particles (i.e., protons and neutrons, confined to $\sim 10^{-6}$ nm) besides electrons. Instead, considering the typical effective masses of electrons in metals and semiconductors, their thermal lengths at room temperature can reach the μm , so they are highly delocalized. The following two sections illustrate two different ways of dealing with Pauli's exclusion principle when modeling crystalline solids, corresponding to two radically different ways of doing quantum mechanics.

Section 2 keeps within the framework of *first quantization*. It is assumed that neither electrons (we mean *crystal* electrons, with effective masses) nor holes can be either created or destroyed. There is only one electron in the whole crystal, submitted to a potential which is mainly the juxtaposition of shielded Coulomb terms, due to atomic orbitals located at the crystal's lattice sites. The way Pauli's principle is dealt with is by comparing the one-electron band spectrum with the Fermi level of an ideal free-electron gas (see Nomenclature). The Fermi level is the chemical potential of such a gas. The exclusion principle can make it so high that for white dwarfs and neutron stars, the pressure it generates prevents the system from becoming a black hole. But the quantum correlation we are concerned with in this section is not Pauli's principle but the overlap between atomic orbitals, usually neglected in simple tight-binding calculations of band structure. The main assumption of the *tight-binding approach* to band spectra is that atoms in a crystal interact only very weakly. As a consequence, the electron's state vector should not differ very much from that of the plain juxtaposition of atomic orbitals located at the crystal's lattice sites. However, neglecting almost all interaction terms and overlap integrals (atomic states at different lattice sites need not be orthogonal to each other) may be too drastic an approximation. Thus Section 2 is devoted to a thorough discussion of the issue.

Instead, the framework of Section 3 is that of *second quantization*. Again, our view of the crystal is that of tight-binding (atoms do not lose their identities).

² Sadly, the generalized disbelief in the mere existence of atoms just one century ago may have contributed to Ludwig Boltzmann's suicide.

Here we are indeed concerned with Pauli's principle. But we deal with it in the style of quantum field theory, by allowing *at most one* electron of each spin projection per atom. For an electron to move ("hop") one lattice site, it must be *annihilated* at its former host atom and *created* in its nearest neighbor one. The purpose of this section is to illustrate an efficient Monte Carlo scheme that implements this strategy to find the ground state of many-electron systems. Recognizing that electrostatic (Coulomb) interaction between electrons is *not* a weak effect but is simply overwhelmed by Pauli's principle, a popular model of itinerant magnetism (the Hubbard model) adds to its Hamiltonian a repulsion term whenever an atom hosts *two* (opposite spin projection) electrons.

Section 4 explores the boundaries of the concept of solid. Perhaps, it should be regarded as a metaphor of this concept. We illustrate a non-equilibrium spatiotemporal pattern formation process, akin to resonant crystal structures, in arrays of FitzHugh-Nagumo cells.

2. Band spectra in the tight-binding approach: effects of the overlaps between neighboring orbitals

2.1 Quantum mechanics in a nutshell

For the benefit of those readers who are unfamiliar with the standard formalism of quantum mechanics, we review its main facts:

- **Dynamical states are vectors:** one can account for the wavelike behavior of quantum objects (e.g., diffraction of single electrons by two slits) by letting their dynamical state $|\psi\rangle$ belong to a vector space over the complex numbers. In few problems (e.g., addition of angular momenta), this vector space is finite-dimensional. But most problems entail infinite sequences (e.g., energy spectrum of the hydrogen atom) or even a continuum of values (e.g., in the measurement of positions and momenta), so the notion of dimension is replaced by that of *completeness* (*any* state can be spanned in suitable "bases"). By assigning a complex number $\langle\varphi|\psi\rangle$ (their "internal product") to every pair of dynamical states $|\psi\rangle, |\varphi\rangle$, the complete vector space is made into a *Hilbert* space.
- **Probabilistic interpretation:** if $|\psi\rangle = \sum_I \alpha_I |\psi_I\rangle$ (be aware that the index set I may be infinite or may even be a patch of \mathbb{R}^d), then $|\alpha_I|^2$ yields the probability to find an outcome represented by $|\psi_I\rangle$, when the system is in state $|\psi\rangle$. This obviously requires normalization: $\langle\psi|\psi\rangle = 1$.
- **Dynamical magnitudes are linear operators L ,** which take a vector into another vector. For instance, the projector $P_\varphi := |\varphi\rangle\langle\varphi|$ projects state $|\psi\rangle$ onto $|\varphi\rangle$. Measuring a dynamical magnitude thus means finding one of its eigenvalues $L|l_I\rangle = l_I|l_I\rangle$. Also of interest is the mean (or expectation) value $\langle\psi|L|\psi\rangle$ of L in a generic state $|\psi\rangle$. Correspondence with classical physics imposes that those eigenvalues be real, and thus dynamical magnitudes must be self-adjoint (Hermitian) operators (P_φ is thus *not* a dynamical magnitude).
- **Unitary evolution:** in order to conserve the probabilistic interpretation, the dynamic evolution of the state is accomplished by a unitary operator. Again, correspondence with classical physics (already implicit in Schrödinger's equation) forces this operator to be $\exp(-iH)$.

- **Wave function:** a possible “basis” set is that of eigenstates ($X|x\rangle = x|x\rangle$) of the position operator, namely, $|\psi\rangle = \int dx \psi(x)|x\rangle$. The *wave function* $\psi(x)$ plays here the role of the coefficients α_I . In modern notation, $\psi(x)$ is written as $\langle x|\varphi\rangle$, so one writes $|\varphi\rangle = \int dx |x\rangle\langle x|\varphi\rangle$.
- **Orthogonality** ($\langle\varphi|\psi\rangle = 0$): a given eigenvalue l_1 of a Hermitian operator L may have a single eigenstate $|l_1\rangle$ (the normalized one out of a dimension-1 subspace over the complex numbers) or more (in this case, it is said to be *degenerate*). Eigenstates corresponding to *different* eigenvalues are *automatically* orthogonal.

2.2 Naive tight-binding approach to band theory

As argued in Section 1, the starting point of this approach is to express the electron’s state vector as a linear combination of atomic orbitals (LCAO) located at the crystal’s lattice sites (we illustrate the procedure in 1D, but clearly, it can be extended to any dimension and lattice symmetry). The eigenvalue problem of the isolated atom centered at x_c is $H_{\text{atom}} |\psi_{\text{atom}}\rangle = E_{\text{atom}} |\psi_{\text{atom}}\rangle$, with $H_{\text{atom}} = T + V(x - x_c)$. We then place a copy $|i\rangle$ of $|\psi_{\text{atom}}\rangle$ centered at each lattice site i ($x_i = ia$) and write the electron’s state in the crystal as LCAO

$$|\psi_{\text{crystal}}\rangle = \sum_i c_i |i\rangle \quad (1)$$

(clearly, $c_i = \langle i|\psi_{\text{crystal}}\rangle$). Now, even though the interatomic distance in the crystal (the “lattice spacing” a) is usually larger than the range x_0 of the atomic orbitals, the atomic cores *do* interact, and one should include at least two effects:

- A *correction* to the isolated atomic level E_{atom} (we shall call α the corrected level)
- Electron tunneling between neighboring orbitals (let γ be a gauge of the energy involved in such a “hopping” process)

It thus makes sense to write up the lattice Hamiltonian in terms of projection operators as

$$H_{\text{crystal}} = \alpha \sum_i |i\rangle\langle i| - \gamma \sum_i (|i+1\rangle\langle i| + |i\rangle\langle i+1|). \quad (2)$$

Two timely comments are:

1. The presence of $|i\rangle\langle i+1|$, the adjoint of $|i+1\rangle\langle i|$, ensures that H_{crystal} be *Hermitian*.
2. The minus sign in the second term ensures crystal stability (energy is released by forming a crystal).

Using Eqs. (1) and (2), the eigenvalue problem $H_{\text{crystal}} |\psi_{\text{crystal}}\rangle = E_{\text{crystal}} |\psi_{\text{crystal}}\rangle$ for the electron in the crystal reads

$$\left[\alpha \sum_i |i\rangle\langle i| - \gamma \sum_i (|i+1\rangle\langle i| + |i\rangle\langle i+1|) \right] \sum_j c_j |j\rangle = E_{\text{crystal}} \sum_j c_j |j\rangle. \quad (3)$$

Assuming the states $|i\rangle$ to be *orthogonal* to each other, the left-hand side of Eq. (3) reads $\sum_i c_i |i\rangle - \gamma \sum_i (c_i |i+1\rangle + c_{i+1} |i\rangle)$. If the number of sites in the crystal is large enough (usually it is $\sim 10^6$), one can greatly simplify the problem by assuming periodic boundary conditions (PBC). This allows to rearrange the sums (their indices become dummy), and Eq. (3) reads $\sum_i [(E_{\text{crystal}} - \alpha)c_i - \gamma \sum_i (c_{i-1} + c_{i+1})] |i\rangle = 0$. Clearly, the LCAO assumes that the $|i\rangle$ are *linearly independent* (be they orthogonal or not), so we are left with the system of difference equations:

$$(E_{\text{crystal}} - \alpha)c_i - \gamma \sum_i (c_{i-1} + c_{i+1}) = 0, i = 1 \dots N \equiv 0. \quad (4)$$

Again invoking PBC, one tries the form $c_j = \exp ijka$ with $-\pi < ka \leq \pi$ (Bloch phase factors) and obtains the known cosine spectrum

$$E_{\text{crystal}} = \alpha - 2\gamma \cos ka, \quad -\pi < ka \leq \pi. \quad (5)$$

What has been left behind? Much indeed:

- We know that α equals E_{atom} plus some correction, but we do not know what the correction is.
- Similarly, we know that γ is the expectation value of the effective potential $W_i := \sum_{j \neq i} V(x - x_j)$ felt by an electron at $x \sim ia$, due to the presence of other atoms. We have kept just $j = i \pm 1$, but even in this approximation, we do not know what the correction is.
- To what extent can one assume the states $|i\rangle$ to be *orthogonal* to each other? This assumption is correct in the absence of interatomic interaction, but not necessarily when atoms interact.

2.3 Tight-binding band calculation: properly done

Recognizing that $H_{\text{crystal}} = \sum_i (H_i^{\text{atom}} + W_i)$ and using Eq. (1), E_{crystal} turns out to be [1, 2]

$$E_{\text{crystal}} = E_{\text{atom}} + \frac{\left[\sum_i \alpha_i |c_i|^2 + \sum_{ij} \gamma_{ij} c_i^* c_j \right]}{\left[\sum_i |c_i|^2 + \sum_{ij} S_{ij} c_i^* c_j \right]}, \quad (6)$$

where

$$\alpha_i := H_{ii} = \langle i | W_i | i \rangle, \gamma_{ij} := H_{ij} = \langle i | W_i | j \rangle, S_{ij} := \langle i | j \rangle, j \neq i. \quad (7)$$

The contribution of the S_{ij} (known as *overlap integrals*) to the band spectrum is our main concern in this section. But not less interesting are that of the α_i terms—which, as argued, shift the electronic energy in an atom from its isolated value E_{atom} , as a collective effect of the other atoms—and that of the γ_{ij} . The latter can be regarded as the sum of two contributions, as $V_j := V(x - x_j)$ can be singled out from W_i . Then whereas the two-center integrals $\gamma_{ij}^{(2)} := \langle i | V_j | j \rangle$ involve only sites i and j , the three-center integrals $\gamma_{ij}^{(3)}$ also involve the sum $\sum_{l \neq i, j} V(x - x_l)$ of the potentials

of the remaining atoms in the solid. Hence, the $\gamma_{ij}^{(3)}$ can be interpreted as the collective effect on the overlap between orbitals i and j .

Variation of Eq. (6) with respect to the LCAO coefficients of Eq. (1)—namely, $\partial E_{\text{crystal}}/\partial a_j^* = 0$ —yields $(H_{ij} - E_{\text{crystal}}S_{ij})a_j = 0, \forall j$. Assuming PBC, H_{ij} and S_{ij} are functions only of the interatomic distance na , with $n = |i - j|$. Again using $a_n = \exp inka$ with $-\pi < ka \leq \pi$, Eq. (6) yields

$$E_{\text{crystal}} = E_{\text{atom}} + \left[\alpha + 2 \sum_n H_n \cos nka \right] / \left[1 + 2 \sum_n S_n \cos nka \right]. \quad (8)$$

Note however that the number of multicenter integrals to be computed is immense! Because of that, most tight-binding calculations plainly ignore almost all the multicenter integrals (keeping only those involving nearest neighbors) and neglect orbital non-orthogonality. This way, the familiar cosine spectrum is obtained. Often, multicenter integrals are just regarded as parameters to fit the results of more sophisticated calculations made by other methods at the highest symmetry points of the Brillouin zone.

In the following, we compute *all* the multicenter integrals *exactly* in the framework of a simple model for the atomic potential. The results help get an intuition on the effect on band spectrum of neglecting overlap integrals and distant-neighbor interactions.

2.4 A simple model that yields an exact tight-binding band spectrum

We restrict ourselves to a 1D monoatomic crystal and assume the interatomic distance a to be larger than the effective range of the screened Coulomb potential representing the atomic core. In such a situation, we can approximate the latter by a Dirac δ -function (complete screening up to the scale of the nucleus):

$$V_{\text{crystal}}(x) = -V_0 \sum_n \delta(x - na). \quad (9)$$

The solution to $H_{\text{atom}} |\psi_{\text{atom}}\rangle = E_{\text{atom}} |\psi_{\text{atom}}\rangle$, with $H_{\text{atom}} = -\frac{\hbar^2}{2m} \frac{d^2}{dx^2} - V_0 \delta(x)$, is an exponential function of the form $\psi_{\text{atom}}(x) = \langle x | \psi_{\text{atom}} \rangle = x_0^{-\frac{1}{2}} \exp\left(-\frac{|x|}{x_0}\right)$. Its range x_0 is related to E_{atom} by $-E_{\text{atom}} = \hbar^2/2mx_0^2 = mV_0/2\hbar^2$.

The only two spatial scales involved in this problem are x_0 and the lattice spacing a . The parameter $t = a/x_0$ will thus allow us to follow the formation of energy bands (k -space picture) as atoms get close together (real-space picture). All the multicenter integrals can be computed analytically in terms of t . The results are $S_n = (1 + nt) \exp(-t)$, $\alpha = 2E_{\text{atom}} \exp(-t)/\sinh t$, and $\gamma_n = 2E_{\text{atom}}[n + \exp(-t)/\sinh t] \exp(-nt)$ [3]. We thus get the following closed expression for $\lambda := (E_{\text{crystal}} - E_{\text{atom}})/E_{\text{atom}}$:

$$\lambda(k, t) = [A_0(t) + A_1(t) \cos ka] / [1 + S(t) \cos ka], \quad -\pi < ka \leq \pi, \quad (10)$$

where $A_0 = \exp(-t) \sinh t / [\sinh t \cosh t - t]$, $A_1 = \sinh t / [\sinh t \cosh t - t]$, and $S = [t \cosh t - \sinh t] / [\sinh t \cosh t - t]$ [3].

Explicit evaluation of Eq. (10) at the bottom ($ka = 0$) and top ($ka = \pi$) of the band shows that for $t < 4$, the cosine spectrum of Eq. (5) underestimates both. Moreover, the multicenter integrals neglected in the cosine spectrum shift *unevenly* the top and bottom of the exact spectrum. Hence, the approximation performs worse for the top than for the bottom of the band.

3. Quantum Monte Carlo method for systems with strongly correlated fermions

3.1 Quantum *statistical* mechanics in a nutshell

The *state vectors* dealt with in Section 1 represent *pure* states. They are the ones which display the spectacular effects seen in recent experiments. Since in this section, we will allow *creation annihilation* of electron states, we must work in the framework of the *grand canonical ensemble*.³ When one deals with *statistical ensembles* of quantum states, the object of interest is the Hermitian operator $\exp(-\beta H)$, called the *density matrix* operator (here $\beta := (k_B T)^{-1}$ and $k_B = R/N_A$ are Boltzmann's constant).

What drives our interest in the *density matrix*—namely, the matrix elements between pure states of $\exp(-\beta H)$ —is the fact that it can be used to find the ground state of many-body systems by stochastic methods. For β large enough, $\exp(-\beta H)$ acts effectively as a *projector* over the lowest-lying energy eigenstate to which the initial (trial) state $|\varphi\rangle$ is not definitely orthogonal. Let E be the corresponding eigenvalue, and consider another trial state $|\chi\rangle$ over which we will project the result. Then we may numerically compute E from

$$\exp(-\Delta\beta E) = \lim_{\beta \rightarrow \infty} [\langle \chi | \exp[-(\beta + \Delta\beta)H] | \varphi \rangle / \langle \chi | \exp(-\Delta\beta H) | \varphi \rangle]. \quad (11)$$

But what is yet more interesting is that in the process, we find a good estimate of the eigenstate itself, namely, its composition in terms of a known basis.

3.2 Monte Carlo pursuit of the ground state

The first step in this computation is to divide the interval $[0, \beta]$ into L “time” slices of width $\Delta\tau = \beta/L$. Some comments are in order:

- a. We take our language from the formal analogy between the density matrix and the evolution operators.
- b. Note that in our case, $\exp(-\beta H)$ is *not meant to be traced over* as it should be in a thermodynamic calculation: here it must rather be considered as a formal tool to make sense in the limit $\beta \rightarrow \infty$.
- c. We may call $U = \exp(-\Delta\tau H)$ the *transfer matrix* operator.

If we can decompose H into a sum of several terms H_i which (although not commuting among them) are themselves *sums of commuting terms*, then for L large enough, the error of approximating

$$\begin{aligned} U &= \exp[-\Delta\tau(H_1 + H_2)] = \exp(-\Delta\tau H_1) \exp(-\Delta\tau H_2) \exp\left\{-\frac{(\Delta\tau)^2}{2}[H_1, H_2]\right\} \\ &= U_1 U_2 \left\{1 - \frac{(\Delta\tau)^2}{2}[H_1, H_2] + \dots\right\} \sim U_1 U_2 \end{aligned}$$

would be at most of order $(\Delta\tau)^2$. Hence

³ We have already stated that the Fermi level is the *chemical potential* of an ideal free-electron gas. This concept is peculiar of the *grand canonical ensemble*.

$$\langle \chi | \exp(-\beta H) | \varphi \rangle \sim \langle \chi | (U_1 U_2)^L | \varphi \rangle. \quad (12)$$

In order to evaluate expression (12), we introduce complete sets of states at each time slice.

The clue to quantum Monte Carlo simulation of Eq. (11) resides in evaluating the sums over complete states *by importance sampling*: in order to do that, observe first that we can rather arbitrarily decompose

$$\langle \psi_j | (U_1 U_2)^L | \psi_i \rangle = S_{ij} P_{ij} \quad (13)$$

as the product of a probability times a (complex) number which we will call a “score.” The probability distribution P_{ij} is at our disposal in order to optimize numerical convergence, minimize statistical error, etc. It can be shown that the way to achieve the last goal is by assigning to every matrix element the same score: that is the basis for the so-called *population method*. Here the initial (trial) state is represented by a “population” in which there are n_i copies of state $|\psi_i\rangle$. The latter corresponds to a definite assignment of occupation numbers both in coordinate and spin (always belonging to the Hilbert space of the problem, i.e., compatible with the conserved quantum numbers). To each individual in the population, we apply the evolution operator, thus obtaining a new state after one time slice. That particular matrix element can be decomposed as indicated in Eq. (20) (but being now $S_{ij} = S = \text{const}$). The way in which we implement the P_{ij} is by making as many copies of that particular resulting state as indicated by $\langle \psi_j | (U_1 U_2)^L | \psi_i \rangle / S$. Proceeding this way, we will get a different population after each time slice which we expect to approach successively to one representing the lowest reachable energy eigenstate.

We have not said anything about the way in which we evaluate the alluded matrix elements, besides the fact that we resort to the decomposition (20): if, as we have already assumed, the term H_i can itself be decomposed into mutually commuting terms, we need only to focus on the Hilbert space of that (much smaller) system. We can compute exactly the matrix elements of the evolution operator for that cluster, write them as the product of a probability times a score (now we can choose the probability distribution to minimize total computing time), and make transitions among cluster states according to those probabilities, assigning then the corresponding score to the particular transition.

3.3 The case of fermions

Again within the *tight-binding approach* to crystalline solids, quantum *creation* (c_{is}^\dagger) and *annihilation* (c_{is}) operators determine the existence of electrons with spin projection σ at site i . For the state vector of the whole set of electrons in the crystal to be totally antisymmetric under exchange, those operators must *anticommute* with each other, unless they refer to the same site and spin projection. In such a case, there can be *at most one* electron per site and spin projection, as required by Pauli’s principle.

In the case of the 1D Hubbard model, we chose the following decomposition of the Hamiltonian, which allows us to consider clusters of only two sites:

$$\begin{aligned} H_1 &= -t \sum_{\text{odd}j} \sum_{\sigma} \left(c_{j+1\sigma}^\dagger c_{j\sigma} + h.c. \right) = -t \sum_{\text{odd}j} \sum_{\sigma} h_{j,j+1} \\ H_2 &= -t \sum_{\text{even}j} \sum_{\sigma} \left(c_{j+1\sigma}^\dagger c_{j\sigma} + h.c. \right) = -t \sum_{\text{even}j} \sum_{\sigma} h_{j,j+1} \end{aligned} \quad (14)$$

$$H_3 = -t \sum_{\text{all } j} n_{j\uparrow} n_{j\downarrow}.$$

The corresponding matrix elements are then $\langle \psi_{i+1} | U_3 U_2 U_1 | \psi_i \rangle$ with $U_1 = \prod_{\text{odd } j} \exp(-\Delta\tau h_{j,j+1})$, $U_2 = \prod_{\text{even } j} \exp(-\Delta\tau h_{j,j+1})$, $U_3 = \prod_j \exp(-\Delta\tau n_{j\uparrow} n_{j\downarrow})$, and

$$\begin{aligned} \langle 01 | \exp(-\Delta\tau h_{j,j+1}) | 01 \rangle &= \langle 10 | \exp(-\Delta\tau h_{j,j+1}) | 10 \rangle = \cosh \Delta\tau, \\ \langle 10 | \exp(-\Delta\tau h_{j,j+1}) | 01 \rangle &= \langle 01 | \exp(-\Delta\tau h_{j,j+1}) | 10 \rangle = \sinh \Delta\tau, \\ \langle 00 | \exp(-\Delta\tau h_{j,j+1}) | 00 \rangle &= \langle 11 | \exp(-\Delta\tau h_{j,j+1}) | 11 \rangle = 1, \end{aligned} \quad (15)$$

from which we write up the (a priori) transition probabilities. Then, in case there is only one occupied site in the block, we draw a random number r and compare it with the a priori transition probability p for the state to remain the same. In case that $r > p$, we make a hopping, i.e., exchange empty and occupied states in the block.

The a priori probabilities can be better chosen if we take into account the occupation of those same two sites by electrons with the other spin projection, thus anticipating to the fact that they will penalize doubly occupied sites [4, 5]. This will certainly improve convergence.

4. Non-equilibrium routes to soft solids

Up to now, we have dealt with crystalline solids. This means that disregarding the *topology*⁴ of the interaction network, we paid attention to the underlying *geometry* of the quantum problem. At present, a host of synthetic materials has outperformed metals at their initial tasks. Some of them still display a varying degree of crystalline character, but others are not crystalline at all. Vulcanized rubbers are an example: created by forcing random chemical bonds in a melt (a “spaghetti dish”), they are inhibited to flow, and, thus, they are amorphous solids.⁵ But they exhibit a varying degree of viscoelastic behavior. In the last decades, the vast discipline of *soft condensed matter* has incorporated to mainstream research in solid-state physics, at equal footing with crystalline solids. The scope of soft condensed matter is very wide. In particular, it considers many non-equilibrium routes to *self-assembled emergent* structures. Of huge interest is the neocortex (not just because understanding the brain’s behavior is one of the “Holy Grails” of science, but because in doing it we may achieve to master a computational strategy which is far more efficient than the present one).

We devote this section to the emergence of non-equilibrium routes to spatio-temporal patterns in an assembly of model “neurons” which keep their essential trait, namely, *excitability*. Admittedly, here the interaction network has the *topology* of a lattice, but here it is not the underlying geometry that is at stake. What does matter here is that the boundary condition be compatible with the interaction, a fact that contributes to the network’s topology.

⁴ It will be a lattice only if all interactions but nearest neighbor ones are neglected. Note that crystals may even have a Cayley tree structure, like the so-called “Bethe lattices.”

⁵ The electronic properties of amorphous solids are also of interest, e.g., in the photovoltaic (PV) industry.

4.1 The non-equilibrium potential (NEP)

It is often hard to tell to what extent an innovation embodies a paradigm shift, for the high diversity (both in scope and extent) of innovations. The formalism of quantum mechanics can be regarded as such—with respect to the Newtonian paradigm—despite the strict correspondence between commutator and Poisson bracket Lie algebras. Also can Einstein’s three papers in his “annus mirabilis” be considered as such, for they demolished our former conceptions of time, of the nature of particles and waves, and of a clockwork universe. In 1908, Paul Langevin supplemented the Newtonian paradigm by letting the forces be of stochastic nature [6]. It is up to your taste to call this innovation a paradigm shift: it definitely abolished our clockwork universe conception and opened up a new chapter in the theory of differential equations. The resulting paradigm is well suited to the current situation, urged by the challenges of nanoscience (where the “systems” are submitted to strong ambient fluctuations) and favored by the increasing parallelism of computational architectures (the simulation schemes are essentially local).

The modern approach to continuous-time dynamic flows is of *first order*.⁶ Given an initial state x_i of a continuous-time, dissipative, autonomous dynamic flow $\dot{x} = f(x)$, its conditional probability density function (PDF) $P(x, t|x_i, 0)$ when submitted to a (Gaussian, centered) white noise $\xi(t)$ with variance γ , namely,

$$\dot{x} = f(x) + \xi(t), \text{ with } \langle \xi(t) \rangle = 0 \text{ and } \langle \xi(t)\xi(t') \rangle = 2\gamma\delta(t - t') \quad (16)$$

obeys the Fokker-Planck equation (FPE):

$$\partial_t P(x, t|x, 0) + \partial J(x, t|x, 0) = 0, \text{ with } J(x, t|x, 0) = D^{(1)}P - \partial_x \left[D^{(2)}(x)P \right] \quad (17)$$

in terms of the “drift” $D^{(1)} = f(x)$ and “diffusion” $D^{(2)} = \gamma$ Kramers-Moyal coefficients. Being the flow nonautonomous but dissipative, one can expect generically situations of statistical energy balance in which the PDF becomes stationary, $\partial_t P_{st}(x) = 0$, thus *independent of the initial state*. Then by defining the *non-equilibrium potential* $\Phi(x) := - \int_{x_0}^x f(y)dy$, it is immediate to find

$$P_{st}(x) = N(x_0) \exp [-\Phi(x)/\gamma]. \quad (18)$$

For n -component dynamic flows, $\Phi(\mathbf{x})$ is defined as $-\lim_{\gamma \rightarrow 0} \gamma \ln P_{st}(\mathbf{x}; \gamma)$ [7], but finding it ceases to be a straightforward matter.⁷ The purpose of this section is to illustrate its *usefulness* when known. It is a *Lyapunov function* for the deterministic dynamics, and the barriers for activated processes can be straightforwardly computed $\lim_{\gamma \rightarrow 0} \gamma \ln$.

4.2 The FitzHugh-Nagumo model and its NEP

Neurons communicate with each other through “action potentials,” which are pulsed variations in the polarization of their membranes. The celebrated Hodgkin-Huxley model of neural physiology was one of the great scientific achievements of the past century. When the goal is insight, however, it is too cumbersome a model

⁶ Recall it was Hamilton who first succeeded in casting conservative systems as first-order ones. In so doing, he put *coordinates* and *momenta* on the same footing. Systems are *conservative* if their phase space does not contract.

⁷ A key is to ensure the multidimensional version of $D^{(2)}$ (a symmetric tensor) to be *nonsingular*.

to work with. A caricature of this model which nonetheless stresses its essence is thus far more desirable in many situations. The FitzHugh-Nagumo model is the minimal model capable to produce *action potentials*, and the key to this behavior is *excitability*. In its minimal expression, the FHN model reads

$$\begin{aligned}\dot{u} &= f(u) - v, \\ \dot{v} &= \epsilon(\beta u - v).\end{aligned}\tag{19}$$

The *activator* field u relaxes very fast and displays *autocatalytic* dynamics (the more there is, the more it produces, but in a *nonlinear* fashion) as needed to produce an action potential. Its *nullcline* $v = f(u)$ (the locus of $\dot{u} = 0$) is a decreasing S-shaped (typically cubic) curve. On the other hand, the *inhibitor* or recovery field v relaxes very slowly (it mimics the time-dependent conductance of the K^+ channels in the axon membrane), so in the end, it enslaves the dynamics. Parameter ϵ is usually very large, to account for the large difference in relaxation rates. Calling λ_1 and λ_2 the eigenvalues of the diffusion tensor, the NEP for the *autonomous* system described by Eq. (19) is [8]

$$\Phi(u, v) = \lambda_2^{-1}(\beta u - v)^2 + (\lambda_1 \epsilon)^{-1} \left(\beta u^2 - 2 \int_{u_0}^u f(x) dx \right)^2.\tag{20}$$

For *nonautonomous* cases, one can draw consequences from Eq. (20) as far as the driving is much slower than the involved relaxation times (adiabatic approximation). In the following, we exploit this advantage.

4.3 Arrays of excitable elements

The result (20) has been employed [9–13] to find the optimal noise variance γ for arrays of excitable elements to display *stochastic resonance synchronized behavior* (see Nomenclature). Here, we briefly illustrate one such a case, where the coupling is *inhibitory* (when neuron i fires, neurons $i \pm 1$ are less likely to fire) [14]. Inhibitory coupling is central in the dynamics of neocortical pyramidal neurons and cortical networks, and plays a major role in synchronous neural firing. On the other hand, inhibitory interneurons are more prone to couple through *gap junctions* (diffusive or “electric” coupling) than excitatory ones. In the transition from wake to anesthetic coma, for instance, diffusive coupling of inhibitor fields helps explaining the spontaneous emergence of low-frequency oscillations with spatially and temporally chaotic dynamics.

We consider a ring of N identical excitable FHN cells, with their *inhibitor* fields *electrically* coupled to those of their nearest neighbors. The system is moreover submitted to a common *subthreshold* (see Nomenclature) harmonic signal $S(t)$ and *independent* additive Gaussian white noises in each component and each site, all with the same variance γ .

Numerical simulation of this stochastic system with increasing γ —for appropriate values of the diffusive coupling E between neighboring inhibitor fields—reveals the noise-induced phenomena taking place: *synchronization with the external signal* of the ring’s activity and (imperfect) *spatiotemporal self-organization* of the cells. For an optimal value of γ , a *stochastic resonance* phenomenon takes place, and the degree of *spatiotemporal self-organization*—alternancy between two *antiphase states* (APS)—is maximum.

For very low γ , only small-amplitude and highly homogeneous [$u_i(t) \approx u_j(t)$] subthreshold oscillations (induced by the adiabatic signal) occur around the $S = 0$

rest state. As γ increases, so does the number of cells that become noise-activated during roughly half a cycle of the external signal. For γ even higher, the cells' activity enhances its coherence with the external signal as a consequence of its coupling-mediated self-organization: as one neuron activates, it usually inhibits its nearest neighbors. The outcome of this phenomenon is the APS, which partially arises along the ring during the stage of activation by noise. In this scenario, noise (together with coupling and signal) plays a constructive role. Nonetheless for γ too large, the sync becomes eventually degraded.

4.4 Spatiotemporal pattern formation in arrays of FHN neurons

We exploit the knowledge of the NEP in Eq. (20) to attempt an analytical description of the problem in Section 4.3. The case of *perfect* spatiotemporal self-organization would be equivalent to a two-neuron system with variables $u_1, u_2, v_1,$ and v_2 and PBC. This simple model allows the formation of an *antiphase* state. Since a NEP cannot be easily found for this system—and with the only purpose of calculating barrier heights—we further reduce this description by *projecting the dynamics along the corresponding slow manifolds*:

$$\epsilon\beta u_{1,2} - v_{1,2} + 2E(v_2 + v_1 - v_{1,2}) = 0. \quad (21)$$

The projected two-variable system turns out to be gradient, a situation in which a NEP can always be found. As a consequence of the PBC, the NEP landscape along the slow manifolds is symmetric with respect to the $u_1 = u_2$ line. For $E = 0.5$ and maximum signal amplitude, the system has two *uniform* attractors (both cells inhibited, both cells activated), two APS (with one cell activated and one inhibited) with the *same* value of $\Phi(u_1, u_2)$, four saddles, and one maximum. For $S = 0$ instead, the uniform attractor with both cells activated has collapsed with the maximum, and, hence, two saddles have disappeared.

When the value of $\Phi(u_1, u_2)$ at the uniform attractor, either APS and either corresponding saddle, is plotted as a function of S , one can see the following:

- Near maximum signal, the uniform attractor yields its stability to the APS. From this value of S on, the NEP barrier for the uniform attractor to decay into the APS (a noise-activated process) is small enough.
- Way before minimum signal, each APS collapses with its own saddle.

One then understands the picture: as S increases, whatever of the APS is chosen. As S decreases past the collapse, only the uniform attractor survives. However, the neuron which was activated before has not recovered completely. Hence in the next signal cycle, the other APS is more likely to appear.

5. Conclusions

In Sections 2 and 3, we have discussed the influence of quantum correlations on the formation of tightly bound solids. Section 2 is devoted to the effects of the overlaps and neglected multicenter integrals on tight-binding band spectra. An exact calculation in the framework of a simple atomic model has shown that they shift *unevenly* the top and bottom of the band spectrum (their effects are more pronounced at the top). Section 3 introduced a quantum Monte Carlo method specific for strongly correlated fermion systems. Section 4 addressed the stochastic

dynamics of a ring of FHN cells—with nearest neighbor *electric* (diffusive) coupling between their *inhibitor* fields—undergoing spatiotemporal pattern formation induced by noise and coupling. By means of a simple model for which a NEP can be found, the mechanism whereby the process takes place was investigated analytically.

Acknowledgements

The author is deeply indebted with his coauthors G.G. Izús, A.D. Sánchez, and M.G. dell'Erba from IFIMAR-CONICET (Faculty of Exact and Natural Sciences) and D.A. Mirabella and C.M. Aldao from INTEMA-CONICET (Faculty of Engineering) of the National University of Mar del Plata (UNMdP), Argentina, with whom he undertook part of the work referred to here. Support by UNMdP, through Grant EXA826–15/E779, is acknowledged.

Nomenclature

Ideal gas	the (identical) particles composing such a gas do not interact between themselves.
Free electrons	they are not submitted to any external (e.g., crystal) potential.
Chemical potential	it is the cost of adding a particle to the system. For two open systems (which can exchange matter and energy with their environments) to come to equilibrium, not only their temperatures but their chemical potentials must be equal.
Subthreshold	unable by itself to drive a transition.
Stochastic resonance	nonlinear systems may display the property of amplifying a <i>subthreshold</i> input signal in the presence of noise with the right intensity.


IntechOpen

Author details

Roberto Raúl Deza
IFIMAR, Faculty of Exact and Natural Sciences, National University of Mar del Plata, CONICET, Argentina

*Address all correspondence to: deza@mdp.edu.ar

IntechOpen

© 2019 The Author(s). Licensee IntechOpen. This chapter is distributed under the terms of the Creative Commons Attribution License (<http://creativecommons.org/licenses/by/3.0>), which permits unrestricted use, distribution, and reproduction in any medium, provided the original work is properly cited. 

References

- [1] Mirabella DA, Aldao CM, Deza RR. Orbital nonorthogonality effects in band structure calculations within the tight-binding scheme. *American Journal of Physics*. 1994;**62**:162-166. DOI: 10.1119/1.17637
- [2] Mirabella DA, Aldao CM, Deza RR. Effects of orbital nonorthogonality on band structure within the tight-binding scheme. *Physical Review B: Condensed Matter*. 1994;**50**:12152-12155. DOI: 10.1103/PhysRevB.50.12152-12155
- [3] Mirabella DA, Aldao CM, Deza RR. Exact one-band model calculation using the tight-binding method. *International Journal of Quantum Chemistry*. 1998; **68**:285-291. DOI: 10.1002/(SICI)1097-461X(1998)68:4<285::AID-QUA6>3.0.CO;2-R
- [4] Kung D, Dahl D, Blankenbecler R, Deza RR, Fulco JR. New stochastic treatment of fermions with application to a double-chain polymer. *Physical Review B*. 1985;**32**:2022-2029. DOI: 10.1103/PhysRevB.32.2022
- [5] Braunstein LA, Deza RR, Mijovilovich A. Exact versus quantum Monte Carlo analysis of the groundstate of the one-dimensional Hubbard model for finite lattices. In: Cordero P, Nachtergaele B, editors. *Nonlinear Phenomena in Fluids, Solids and Other Complex Systems*. Amsterdam: North-Holland; 1991. pp. 313-327. DOI: 10.1016/B978-0-444-88791-7.50024-7
- [6] Lemons D. Paul Langevin's 1908 paper "On the theory of Brownian motion" ("Sur la théorie du mouvement brownien," *C. R. Acad. Sci. (Paris)* 146, 530-533 (1908)). In: *AIP Conference Proceedings*, Vol. 65. 1997. pp. 1079-1081. DOI: 10.1119/1.18725
- [7] Graham R. Weak noise limit and nonequilibrium potentials of dissipative dynamical systems. In: Tirapegui E, Villarroel D, editors. *Instabilities and Nonequilibrium Structures*. Dordrecht: D. Reidel; 1987. pp. 271-290. DOI: 10.1007/978-94-009-3783-3_12
- [8] Izús GG, Deza RR, Wio HS. Exact nonequilibrium potential for the FitzHugh–Nagumo model in the excitable and bistable regimes. *Physical Review E*. 1998;**58**:93-98. DOI: 10.1103/PhysRevE.58.93
- [9] Izús GG, Deza RR, Wio HS. Critical slowing-down in the FitzHugh–Nagumo model: A non-equilibrium potential approach. *Computer Physics Communications*. 1999;**121-122**: 406-407. DOI: 10.1016/S0010-4655(99)00368-9
- [10] Wio HS, Deza RR. Aspects of stochastic resonance in reaction–diffusion systems: The nonequilibrium-potential approach. *European Physical Journal: Special Topics*. 2007;**146**:111. DOI: 10.1140/epjst/e2007-00173-0
- [11] Izús GG, Deza RR, Sánchez AD. Highly synchronized noise-driven oscillatory behavior of a FitzHugh—Nagumo ring with phase-repulsive coupling. *AIP Conference Proceedings*. 2007;**887**:89-95. DOI: 10.1063/1.2709590
- [12] Izús GG, Sánchez AD, Deza RR. Noise-driven synchronization of a FitzHugh–Nagumo ring with phase-repulsive coupling: A perspective from the system's nonequilibrium potential. *Physica A: Statistical Mechanics and its Applications*. 2009;**388**:967-976. DOI: 10.1016/j.physa.2008.11.031
- [13] Sánchez AD, Izús GG. Nonequilibrium potential for arbitrary-connected networks of FitzHugh–Nagumo elements. *Physica A: Statistical Mechanics and its Applications*. 2010; **389**:1931-1944. DOI: 10.1016/j.physa.2010.01.013

[14] Sánchez AD, Izús GG, Dell'Erba MG, Deza RR. A reduced gradient description of stochastic-resonant spatiotemporal patterns in a FitzHugh–Nagumo ring with electric inhibitory coupling. *Physics Letters A*. 2014;**378**: 1579-1583. DOI: 10.1016/j.physleta.2014.03.048

IntechOpen

IntechOpen